Electronic Supplementary Information

Synthesis of unconventional Pd-Se nanoparticles for phase-dependent ethanol electrooxidation

Zhenya Hu,[ab] Niuwa Yang,[ab] Yongjun Feng,[c] Lin Xu,[d] Chaoquan Hu,[ae] Hui Liu,*[ae] Shaonan Tian,*[a] Jun Yang*[abe]

[a]*State Key Laboratory of Multiphase Complex Systems, Institute of Process Engineering, Chinese Academy of Sciences, Beijing 100190, China. Email: liuhui@ipe.ac.cn (H.L.); sntian@ipe.ac.cn (S.T.); jyang@ipe.ac.cn (J.Y.)*

[b]*Center of Materials Science and Optoelectronics Engineering, University of Chinese Academy of Sciences, Beijing 100049, China*

[c]*State Key Laboratory of Chemical Resource Engineering, Beijing Engineering Center for Hierarchical Catalysts, College of Chemistry, Beijing University of Chemical Technology, No. 15 Beisanhuan East Road, Beijing 100029, China*

[d]*School of Chemistry and Materials Science, Jiangsu Key Laboratory of New Power Batteries, Jiangsu Collaborative Innovation Centre of Biomedical Functional Materials, Nanjing Normal University, Nanjing 210023, P. R. China*

[e]*Nanjing IPE Institute of Green Manufacturing Industry, Nanjing 211100, Jiangsu, China*

Experimental

Materials

$Pd(acac)_2$ (99.5%), oleylamine (OLA, 95%), $NaBH_4$ (98%) were purchased from Sigma-Aldrich and used as received. Se powder (99.7%) was obtained from Fuchen (Tianjin) Chemical Reagent Co., Ltd. Ethanol (99.7%), n-hexane (>99.5%) were bought from Sinopharm Chemical Reagent Co., Ltd. Nafion solution (5% in a mixture of lower aliphatic alcohols and water) from Sigma-Aldrich, Vulcan XC-72 carbon powder (BET specific surface area is 250m^2 g^{-1}, and the average particle size is 40 ~ 50 nm) from Cabot, and commercial Pd/C catalyst (20 wt% of Pd, and ca. 3 nm Pd nanoparticles supported on Vulcan XC-72 carbon) from Johnson Matthey, were used as received. All glassware and magnets were cleaned with aqua regia, followed by copious rinsing with deionized water before drying in an oven.

Methods

Synthesis of $PdSe_2$, $Pd_{17}Se_{15}$ and Pd_7Se_2 nanoparticles

In a typical preparation of Pd-Se NPs with the $PdSe_2$ phase, 15.3 mg of $Pd(acac)_2$ (0.05 mmol) was dissolved in 5 ml of OLA. The Se solution was prepared by dissolving 10 mg of Se powder (0.125 mmol) and 10 mg of $NaBH_4$ (0.25 mmol) in 5 mL of OLA. The Se precursor was injected quickly into the Pd-containing reaction mixture, and then heated to 120°C and maintained there for 40 min under N_2 flow. Subsequently, the reaction system was heated to 200°C for another 30 min and cooled down to room temperature naturally afterwards. The synthesis of Pd-Se NPs with the $Pd_{17}Se_{15}$ phase was achieved by using similar procedure but changing the amount of Se and $NaBH_4$ to 5.0 mg and 5.0 mg, while the Pd-Se NPs with the Pd_7Se_2 phase were obtained by changing the amount of Se and $NaBH_4$ to 1.5 mg and 1.5 mg, respectively. The products were collected by centrifugation and washed with ethanol/n-hexane three times before final dispersion in 10 mL of n-hexane.

Characterization

The transmission electron microscopy (TEM) and high-resolution TEM (HRTEM) were performed at a JEOL JEM-2010F electron microscope, and an energy dispersive X-ray spectroscopy (EDX) analyzer attached to the TEM was used to detect the relevant elements in the as-prepared samples. Powder X-ray diffraction (XRD) patterns were recorded on a SmartLab (9KW) using Cu Kα radiation (λ=0.154056 nm), while X-ray photoelectron spectroscopy (XPS) was conducted on a VG ESCALAB MKII spectrometer for characterizing the chemical states of the relevant elements.

Electrochemical measurements

For the electrochemical measurements, all relevant samples were loaded on the XC-72 carbon substrate. The calculated amounts of carbon powder were added to the n-

hexane solution of the as-prepared samples. After stirring for 6 h, the carbon supported samples were collected by centrifugation and dried at room temperature in a vacuum. The accurate contents of the Pd loaded on carbon substrates were determined by ICP-AES.

Electrochemical measurements were conducted on a standard three-electrode cell that was connected to a Bio-logic VMP3 potentiostat. A leak-free Ag/AgCl electrode and a platinum mesh (1×1 cm^2) attached to a platinum wire were used as the reference and counter electrode, respectively. All potentials were converted to values with reference to RHE. The catalyst inks were prepared as following: 5 mg of the above catalysts were dispersed ultrasonically into a mixed solution containing 0.8 mL of ethanol, 0.15 mL of water and 0.05 mL of Nafion solution. Then, 5 μL of the ink was dropped onto the glassy carbon electrode with a diameter of 5 mm (electrode area was 0.196 cm^2), followed by drying in a stream of warm air at 70 ℃. And the electrode was connected to a three-electrode test system to measure the electrochemical properties.

Electrochemically active surface areas (ECSAs) of these Pd-based nanoparticles were determined from CVs in the area of PdO reduction peaks with a scan of 50 mV s^{-1}, and were calculated using an equation in term of ECSA= Q/0.405G, where Q is the charge by integrated the reduction peak area of PdO to Pd (mC), G represents the mass loading of Pd on the electrode determined by ICP-AES, and 0.405 is the theoretical charge (mC cm^{-2}) for the reduction of Pd. For CO stripping tests, the work electrode was immersed in 1 M KOH solution. Then, CO was purged in the solution for 30min to achieve the maximum coverage of CO. The modified electrode was quickly moved to a fresh N_2 saturated 1 M KOH solution, and the CO stripping voltammogram was recorded between -1–0.2 V versus Ag/AgCl was scanned at a rate of 50 mV s^{-1}.

The catalytic performance of the $PdSe_2$, $Pd_{17}Se_{15}$, Pd_7Se_2, and commercial Pd/C catalyst for the ethanol oxidation was measured at room temperature by cyclic voltammetry (CV) and chronoamperometry (CA). For these measurements, the potential window of -1–0.2 V versus Ag/AgCl was scanned at a rate of 50 mV s^{-1}. The electrolyte was 1 M KOH containing 1 M ethanol.

Table S1. The structural parameters of the as-prepared Pd-Se NPs by wet-chemistry method.

Chemical formula	$PdSe_2$	$Pd_{17}Se_{15}$	Pd_7Se_2
Crystal system	orthorhombic	cubic	monoclinic
Space group	Pbca(61)	Pm-3m (221)	P21/c(14)
Unit cell parameters	a = 5.7 Å, b = 5.8 Å, c = 7.7 Å, α = β = γ =90˚, V = 257.8 Å^3	a = b = c = 10.6 Å, α = β = γ =90˚, V = 1185.6 Å^3	a = 9.5 Å, b = 5.4 Å, c = 5.5 Å, α = γ=90˚, β = 86.5˚, V = 278.2 Å^3
Z	4	2	2

Table S2. The ECSAs of $PdSe_2$, $Pd_{17}Se_{15}$, Pd_7Se_2 NPs and commercial Pd/C catalyst, and their corresponding Pd content determined by ICP-AES.

Catalyst	ECSA (m^2 g^{-1})	The content of Pd in the catalyst (%)
$PdSe_2$	18.7	7.4
$Pd_{17}Se_{15}$	30.4	11.3
Pd_7Se_2	29.2	10.6
Pd/C	35.6	18.0

Table S3. Electrochemical measurements of ethanol oxidation on $PdSe_2$, $Pd_{17}Se_{15}$, Pd_7Se_2 NPs and commercial Pd/C catalyst.

Catalyst	FPP (V)	I_f (mA cm^{-2} and A mg^{-1})	BPP (V)	I_b (mA cm^{-2} and A mg^{-1}	I_f/ I_b (mass current density)
$PdSe_2$	0.88	29.4/7.2	0.73	26.8/6.6	1.10
$Pd_{17}Se_{15}$	0.86	17.1/5.2	0.74	16.3/5.0	1.04
Pd_7Se_2	0.84	15.4/4.8	0.73	16.2/4.9	0.98
Pd/C	0.88	3.3/1.1	0.75	4.3/1.5	0.73

FPP: Forward peak potential; I_f: Forward peak current density; BPP: Backward peak potential; I_b: Backward peak current density. The data were obtained from Figure 3B and C.

Table S4. EOR performances of Pd-Se NPs and various Pd-based electrocatalysts from published works.

Catalyst	Electrolyte	Mass Activity ($A\ mg_{Pd}^{-1}$)	Specific Activity ($mA\ cm^{-2}$)	rate ($mV\ s^{-1}$)	Ref.
$PdSe_2$ NPs/C	1.0 M KOH + 1.0 M ethanol	7.2	29.4	50	This work
$Pd_{17}Se_{15}$ NPs/C	1.0 M KOH + 1.0 M ethanol	5.2	17.1	50	This work
Pd_7Se_2 NPs/C	1.0 M KOH + 1.0 M ethanol	4.8	15.4	50	This work
Pd aerogel	1.0 M KOH + 1.0 M ethanol	7.83	\	50	Ref. 1
PdRu-NiZn oxyphosphide	1.0 M KOH + 1.0 M ethanol	4.72	12.3	50	Ref. 2
$Pd@Pt_3Ni$	1.0 M KOH + 1.0 M ethanol	5.78	13.61	50	Ref. 3
Pd_7Ru_1 nanodendrites	1.0 M KOH + 1.0 M ethanol	1.15	~7	50	Ref. 4
PdCuCo alloy	1.0 M NaOH +1.0 M ethanol	3.95	7.0	50	Ref. 5
Pd nanocages with Bi doping	1.0 M KOH + 1.0 M ethanol	3.49	10.37	50	Ref. 6
PdIn	1.0 M KOH + 1.0 M ethanol	2.82	\	50	Ref. 7
c-Pd-Ni-P@ *a*-Pd-Ni-P	1.0 M KOH + 1.0 M ethanol	3.05	~11	50	Ref. 8
PdAg nanowires	1.0 M KOH + 1.0 M ethanol	2.84	11.2	50	Ref. 9
Au@Pd	1.0 M KOH + 1.0 M ethanol	2.92	\	50	Ref. 10
Pd/B,N-codope graphene	1.0 M NaOH +1.0 M ethanol	2.156	\	50	Ref. 11
Pd-Ni-P	1.0 M NaOH +1.0 M ethanol	4.945	\	50	Ref. 12

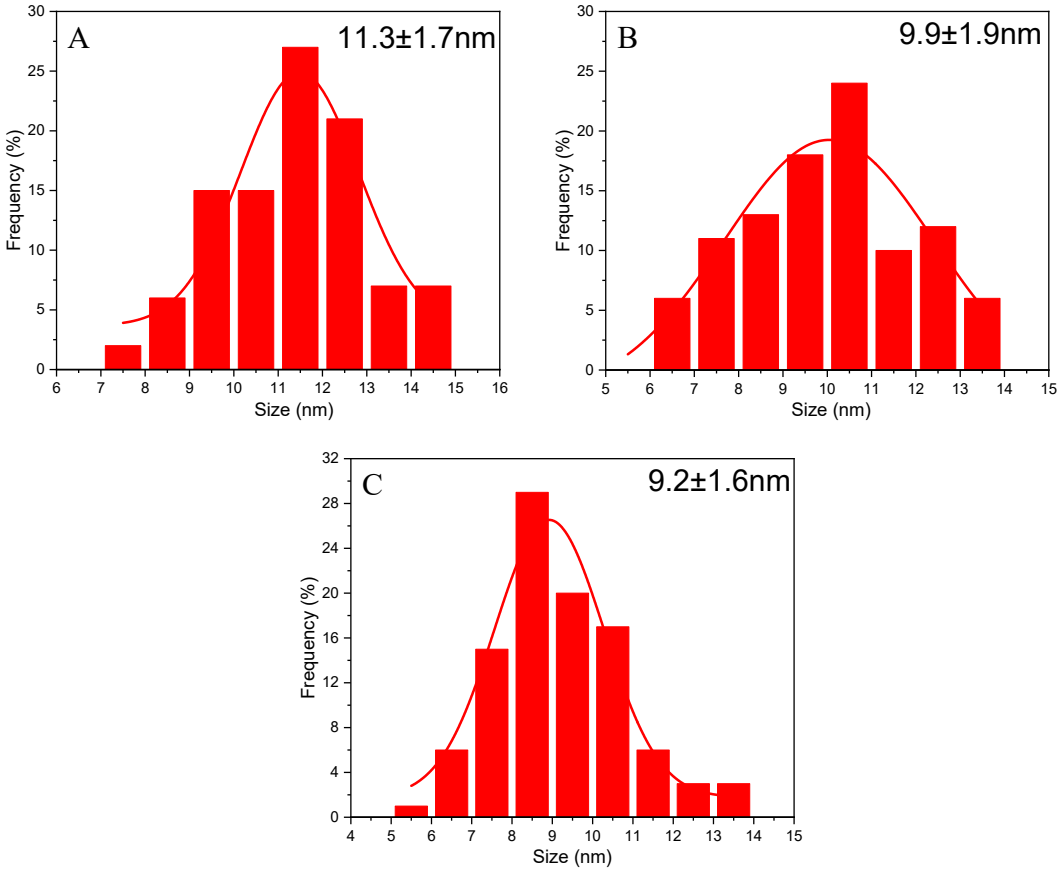

Fig. S1 The Particle Size Histograms of $PdSe_2$ NPs (A), $Pd_{17}Se_{15}$ NPs (B) and Pd_7Se_2 NPs (C), respectively.

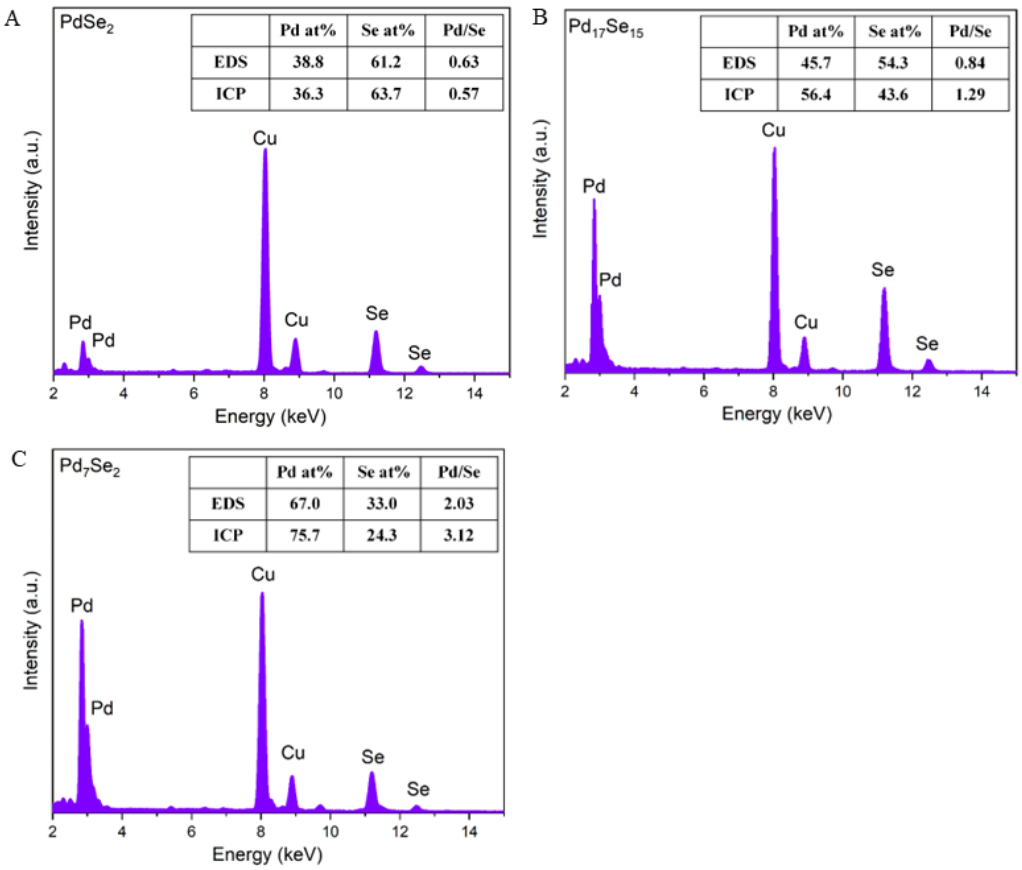

Fig. S2 EDX spectra of the as-prepared $PdSe_2$ NPs (A), $Pd_{17}Se_{15}$ NPs (B) and Pd_7Se_2 NPs (C).

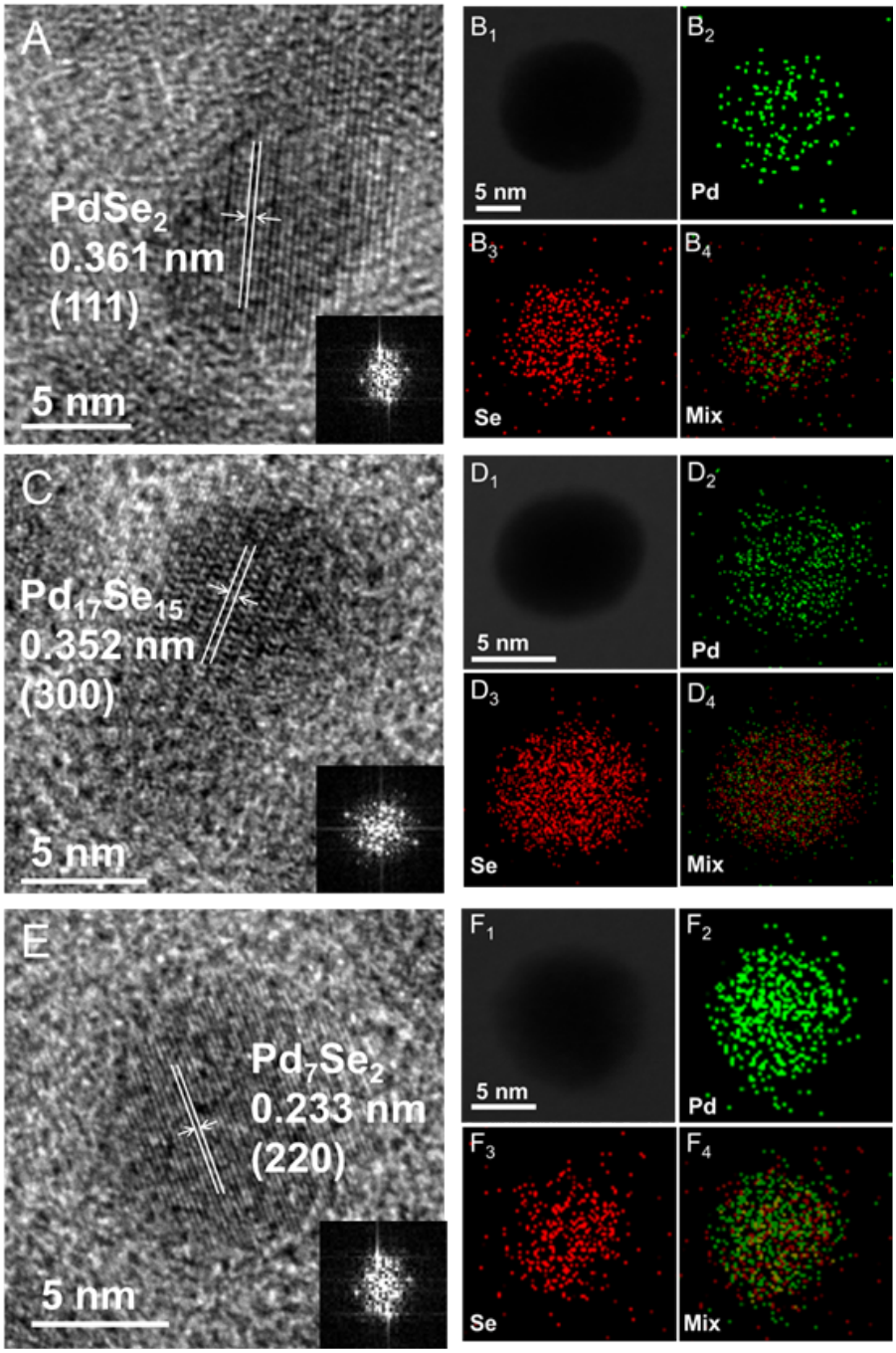

Fig. S3 HRTEM images of the $PdSe_2$ NPs (A), $Pd_{17}Se_{15}$ NPs (C) and Pd_7Se_2 NPs (E), respectively, and the inserts of A, C, and E show the corresponding Fast Fourier Transform (FTT); STEM and corresponding element maps of the $PdSe_2$ NPs (B), $Pd_{17}Se_{15}$ NPs (D) and Pd_7Se_2 NPs (F), respectively.

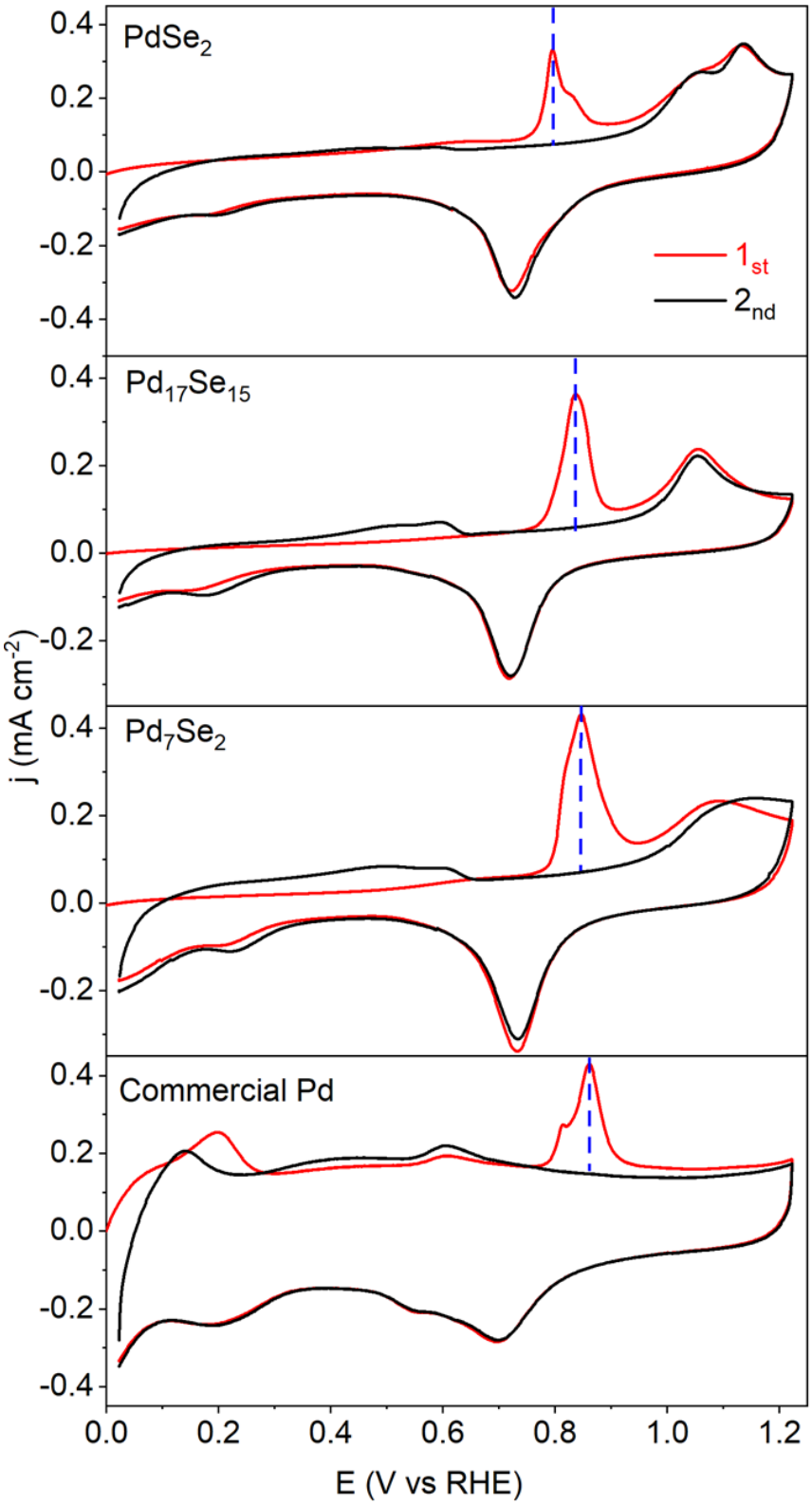

Fig. S4 CO stripping curves over $PdSe_2$, $Pd_{17}Se_{15}$, Pd_7Se_2, and commercial Pd/C catalyst at a scan rate of 50 mV s^{-1} in 1 M KOH solution.

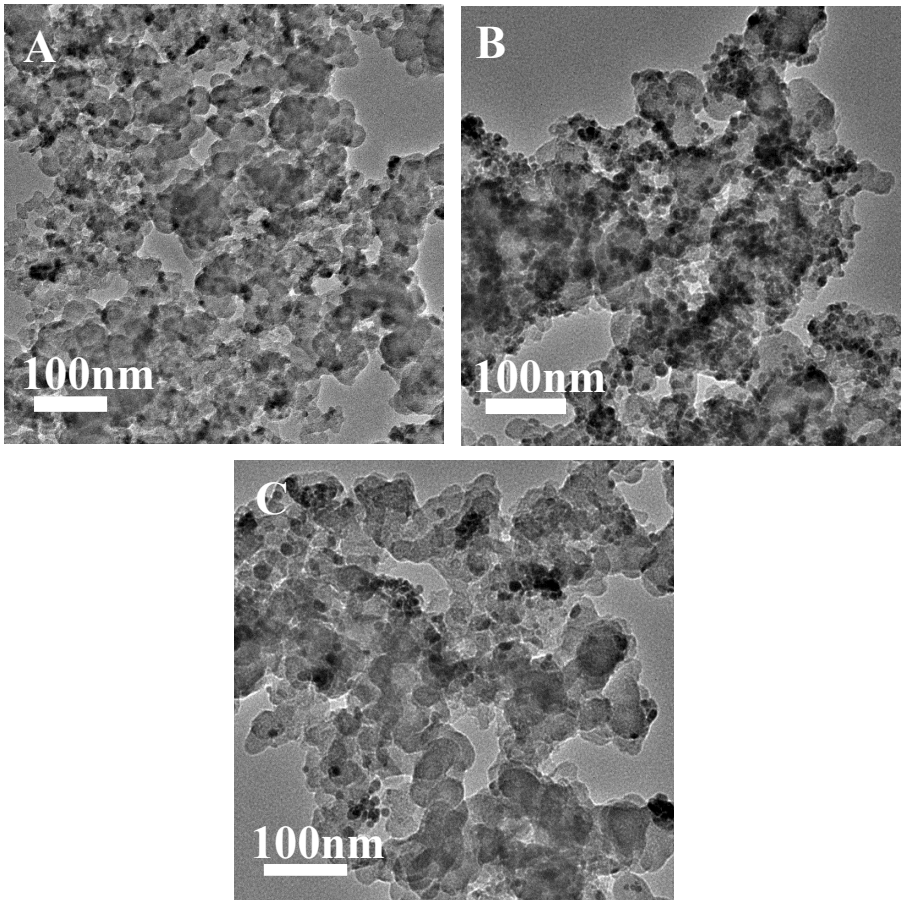

Fig. S5 TEM images of the carbon-supported $PdSe_2$ (A), $Pd_{17}Se_{15}$ (B) and Pd_7Se_2 NPs (C).

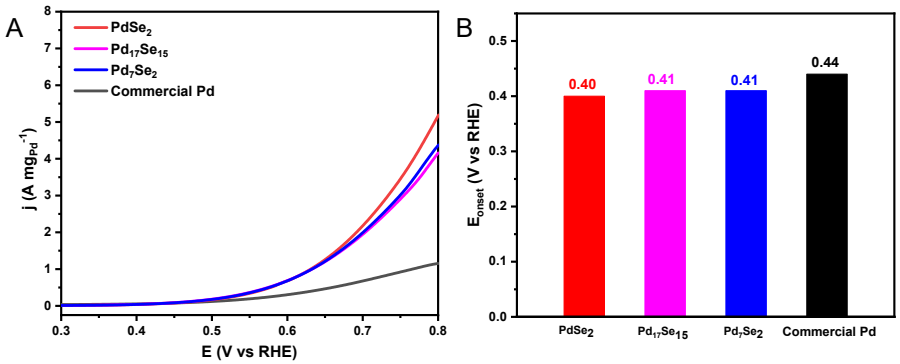

Fig. S6 (A) The local magnified CV curves from 0.3-0.8 V vs RHE in 1 M KOH containing 1 M C_2H_5OH; (B) comparison of onset potentials for $PdSe_2$, $Pd_{17}Se_{15}$, Pd_7Se_2, and commercial Pd/C catalyst.

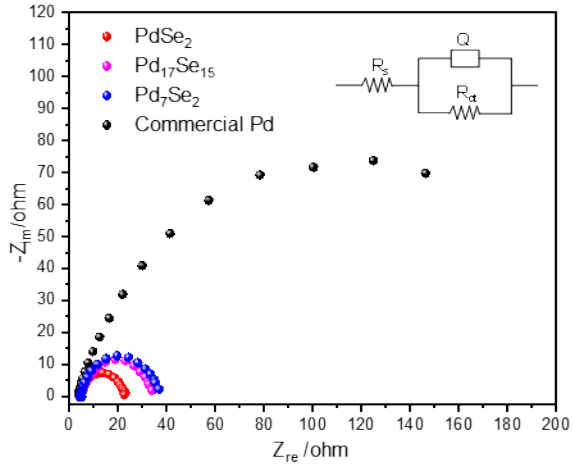

Fig. S7 Nyquist plots of $PdSe_2$, $Pd_{17}Se_{15}$, Pd_7Se_2 and commercial Pd catalyst for the ethanol oxidation in 1 M KOH solution containing 1 M ethanol.

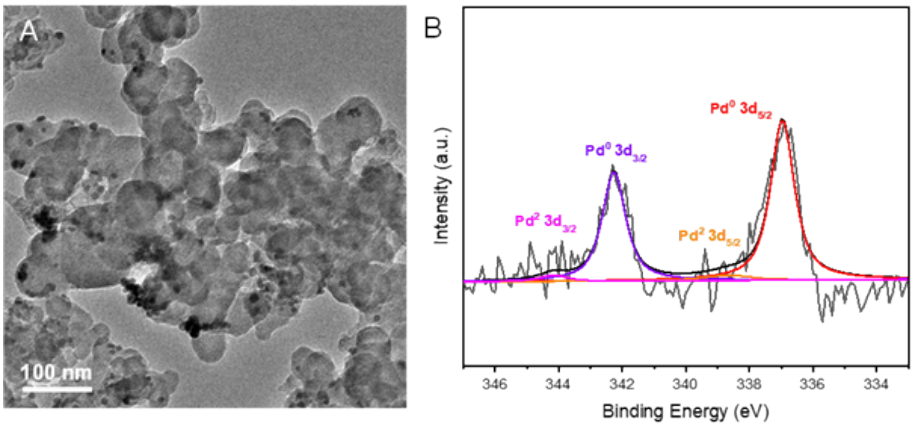

Fig. S8 (A) TEM image of the carbon-supported $PdSe_2$ after the chronoamperometry test; (B) the Pd 3d XPS spectra of the $PdSe_2$ NPs after the chronoamperometry test.

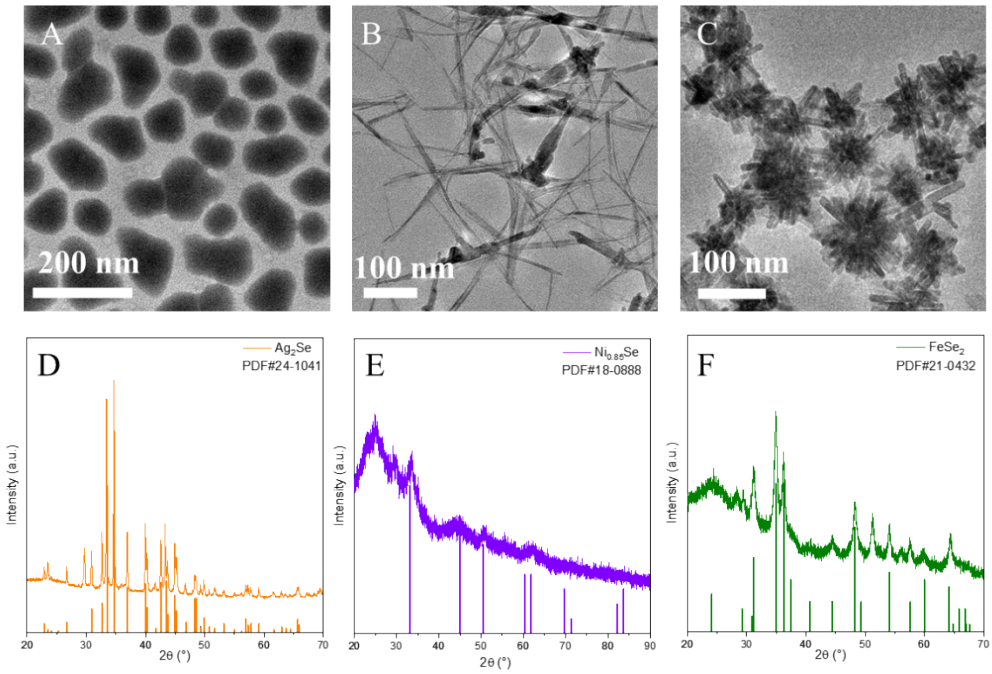

Fig. S9 (A–C) TEM images and (D–F) XRD patterns of the Ag_2Se NPs (A,D), $Ni_{0.85}Se$ NPs (B,E) and $FeSe_2$ NPs (C,F), respectively.

ESI Reference

1. W. Liu, A.-K. Herrmann, D. Geiger, L. Borchardt, F. Simon, S. Kaskel, N. Gaponik and A. Eychmüller, *Angew. Chem. Int. Ed.*, 2012, **51**, 5743.
2. H. Xu, P. Song, Y. Zhang and Y. Du, *Nanoscale*, 2018, **10**, 12605.
3. Y. Wang, W. Wang, F. Xue, Y. Cheng, K. Liu, Q. Zhang, M. Liu and S. Xie, *Chem. Commun.*, 2018, **54**, 5185.
4. K. Zhang, D. Bin, B. Yang, C. Wang, F. Ren and Y. Du, *Nanoscale*, 2015, **7**, 12445.
5. Y. Shu, X. Shi, Y. Ji, Y. Wen, X. Guo, Y. Ying, Y. Wu, and H. Yang, *ACS Appl. Mater. Interfaces*, 2018, **10**, 4743.
6. X. Li, H. You, C. Wang, D. Liu, R. Yu, S. Guo, Y. Wang and Y. Du, *J. Colloid Interf. Sci.*, 2021, **591**, 203.
7. Y.-J. Chen, Y.-R. Chen, C.-H. Chiang, K.-L. Tung, T.-K. Yeh and H.-Y. Tuan, *Nanoscale*, 2019, **11**, 3336.
8. P.-F. Yin, M. Zhou, J. Chen, C. Tan, G. Liu, Q. Ma, Q. Yun, X. Zhang, H. Cheng, Q. Lu, B. Chen, Y. Chen, Z. Zhang, J. Huang, D. Hu, J. Wang, Q. Liu, Z. Luo, Z. Liu, Y. Ge, X.-J. Wu, X.-W. Du and H. Zhang, *Adv. Mater.*, 2020, **32**, 2000482.
9. H. Lv, Y. Wang, A. Lopes, D. Xu and B. Liu, *Appl. Catal. B: Environ.*, 2019, **249**, 116.
10. Y. Chen, Z. Fan, Z. Luo, X. Liu, Z. Lai, B. Li, Y. Zong, L. Gu and H. Zhang, *Adv. Mater.*, 2017, **29**, 1701331.
11. Q. Liu, J. Fan, Y. Min, T. Wu, Y. Lin and Q. Xu, *J. Mater. Chem. A*, 2016, **4**, 4929.
12. L. Chen, L. Lu, H. Zhu, Y. Chen, Y. Huang, Y. Li and L. Wang, *Nat. Commun.*, 2017, **8**, 14136.